

Mass-dependence of the Λ hypernuclear decay widths

G. Garbarino ^{a*}

^aGrup de Física Teòrica, Universitat Autònoma de Barcelona,
08193 Bellaterra, Barcelona, Spain

Two different approaches have been employed for the evaluation of the decay widths of Λ -hypernuclei (ranging from ${}^5_\Lambda\text{He}$ to ${}^{208}_\Lambda\text{Pb}$) with the polarization propagator method. In ref. [1], the two-nucleon stimulated non-mesonic decay, $\Lambda NN \rightarrow NNN$, has been parameterized phenomenologically by means of data on the pion-nucleus optical potential. The other approach [2] consisted in a fully microscopic description of the non-mesonic decays through the first order approximation of the so-called bosonic-loop-expansion. Both calculations reproduce, with approximately the same accuracy, the experimental decay rates for the whole range of mass numbers considered.

1. INTRODUCTION

Because of its kinematics, the decay mode of the free Λ -hyperon, $\Lambda \rightarrow \pi N$, is disfavoured by the Pauli principle if it occurs in nuclear systems. However, the presence of the nuclear medium is responsible for the opening of new, non-mesonic decay channels, $\Lambda N \rightarrow NN$ and $\Lambda NN \rightarrow NNN$. The non-mesonic decay is characterised by large momentum transfers, thus the details of nuclear structure do not have a substantial influence, but the NN and ΛN short range correlations turn out to be very important. Experimental data show an anticorrelation between mesonic and non-mesonic decay modes such that the total lifetime is quite stable over the whole hypernuclear mass spectrum.

2. FRAMEWORK FOR CALCULATION

Within the polarization propagator method the weak decay of Λ -hypernuclei is studied through a many-body description of the hyperon self-energy, whose imaginary part gives the Λ decay width:

$$\Gamma_\Lambda = -2 \operatorname{Im} \Sigma_\Lambda. \quad (1)$$

This technique provides a unified picture of the different decay channels. Moreover, it is alternative and equivalent to the standard wave function method, which makes use of shell model hypernuclear wave functions and pion waves generated by pion-nucleus optical potentials.

Here we only present and discuss the results of our calculations. Details concerning the framework used can be found in refs. [1–3]. The $2p-2h$ part of the irreducible polarization

*The author acknowledges financial support from the EEC through TMR Contract CEE-0169

propagator has been estimated, in ref. [1], by using a *phenomenological* parameterization supplied by the pion–nucleus optical potential, extracted from data on pion absorption in pionic atoms. The phase space available for real $2p-2h$ excitations has also been taken into account, in order to extrapolate the data for off-mass shell pions. The Feynman diagrams contributing to the Λ self-energy in nuclear systems can be classified in a theoretically grounded scheme by using a functional approach, according to the prescriptions of the so-called bosonic-loop-expansion. In ref. [2], a *microscopic* calculation of the non-mesonic decays within the one-boson-loop approximation has been performed.

3. RESULTS

In this section the main results obtained in refs. [1,2] are discussed.

3.1. Phenomenological calculation

The local density approximation, used to extend the calculation made in nuclear matter to finite nuclei, requires the knowledge of the Λ wave function in nuclei. We have obtained these wave functions from Wood–Saxon wells with radius and depth fixed to reproduce the first two single particle states of the hypernuclei considered.

A crucial ingredient in the calculation of the non-mesonic decay rates is the short range part of the strong NN and ΛN interactions. They have been expressed by phenomenological functions, which supply a good reproduction of realistic G –matrix calculations in the NN case. Since 1) there are no experimental indications on the strong ΛN short range interaction and 2) we use a phenomenological picture of the Λ decay which go beyond the description usually employed for processes not involving strangeness, the zero energy and momentum limit, g' and g'_Λ , of the correlation functions have been kept as free parameters. They have been fixed (on the values $g' = 0.8$ and $g'_\Lambda = 0.4$) in order to reproduce the non-mesonic decay rate of ^{12}C .

Then, the calculation has been extended to hypernuclei ranging from $^5\Lambda\text{He}$ to $^{208}\Lambda\text{Pb}$. The result are shown in figure 1. The mesonic rate Γ_M rapidly vanishes with the nuclear mass number A . This is related to the decreasing phase space allowed for the decay and to smaller overlaps between the Λ probability distribution and the nuclear surface, as A increases. The results for Γ_M are in good agreement both with experimental data (included the new ones from KEK presented at this conference [4]) and with other theoretical estimations [5,6], obtained in shell model calculations. With the exception of $^5\Lambda\text{He}$, the two-body induced decay (Γ_2) is rather independent of the hypernuclear dimension and is about 15% of the total width, which is also fairly constant with A . In figure 1 our calculation for non-mesonic and total decay widths ($\Gamma_{NM} = \Gamma_1 + \Gamma_2$ and Γ_T) is compared with recent (after 1990) experimental data [7–11]. The theoretical results are in good agreement with the experiment over the whole hypernuclear mass range explored. In particular, the saturation of the $\Lambda N \rightarrow NN$ interaction in nuclei is well reproduced.

3.2. Microscopic calculation

The results presented in this section have been obtained in ref. [2] within the one-boson-loop (OBL) approximation. The calculation of the OBL diagrams for the Λ self-energy in finite nuclei (using the local density approximation) is not possible here because of the long computing time already for the evaluation of the decay rates at fixed Fermi momentum

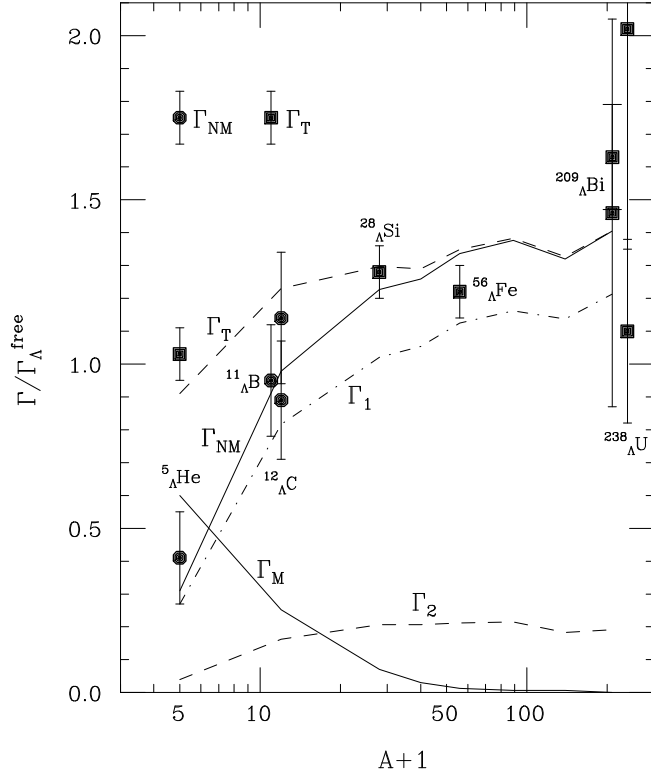


Figure 1. Partial Λ decay widths in finite nuclei as a function of the mass number A .

(namely in nuclear matter). In order to compare the calculation with experimental data, we assigned different “average” Fermi momenta to three mass regions in the hypernuclear spectrum. We used the following prescription:

$$\langle k_F \rangle = \int d\vec{r} k_F(\vec{r}) |\psi_\Lambda(\vec{r})|^2, \quad (2)$$

which derives from weighting the nucleon local Fermi momentum $k_F(\vec{r})$ with the probability density of the Λ inside the nucleus $|\psi_\Lambda(\vec{r})|^2$. We classified the hypernuclei for which experimental data are available into the following mass regions:

- medium-light: $A \simeq 10 \Rightarrow \langle k_F \rangle = 1.1 \text{ fm}^{-1}$;
- medium: $A \simeq 30 \div 60 \Rightarrow \langle k_F \rangle = 1.2 \text{ fm}^{-1}$;
- heavy: $A \gtrsim 200 \Rightarrow \langle k_F \rangle = 1.36 \text{ fm}^{-1}$.

As in the phenomenological approach, the Landau parameters g' and g'_Λ are the only free parameters of the calculation.

In figure 2 we show the dependence of the total non-mesonic width on the Fermi momentum of nuclear matter (we remind that for this range of Fermi momenta, in infinite nuclear matter the mesonic decay is strictly forbidden). Here g'_Λ has been fixed to 0.4, since with this value the experimental data can be reproduced, in ring approximation, by using g' values compatible with the phenomenology of other physical processes. The solid curves refer to the OBL approximation, with $g' = 0.7, 0.8, 0.9$ from the top to the

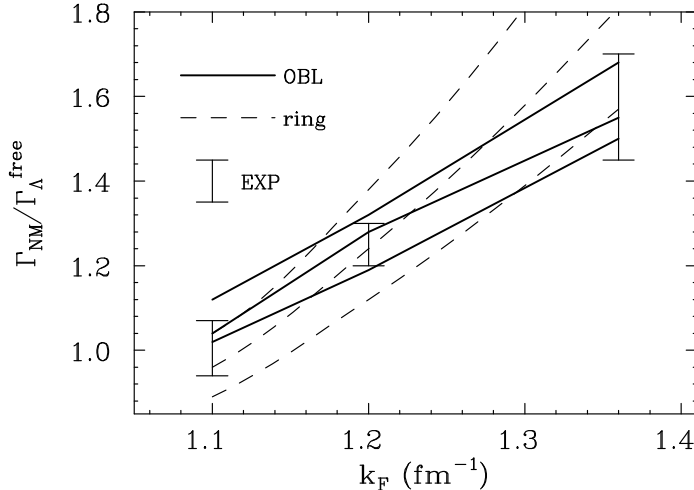


Figure 2. Dependence of the non-mesonic width on the Fermi momentum. The solid curves refer to the one-boson-loop approximation (with $g' = 0.7, 0.8, 0.9$ from the top to the bottom), while the dashed lines refer to the ring approximation ($g' = 0.5, 0.6, 0.7$). Reference experimental bands are also shown.

bottom, while the dashed lines refer to the ring approximation, with $g' = 0.5, 0.6, 0.7$, again from the top to the bottom. We note that the OBL calculation reproduce rather well the data for the three mass regions when $g' = 0.8$. Incidentally, the same value for g' has been employed in the phenomenological calculation. However, one must point out that the role played by the Landau parameters is different in the two approaches we used.

In conclusion, both calculations reproduce, with approximately the same accuracy, the experimental data. This proves the reliability in using 1) averaged Fermi momenta to simulate the Λ decay in finite nuclei and 2) the phenomenological model to describe the non-mesonic decay.

REFERENCES

1. W. M. Alberico, A. De Pace, G. Garbarino and A. Ramos, Phys. Rev. **C 61** (2000) 044314.
2. W. M. Alberico, A. De Pace, G. Garbarino and R. Cenni, Nucl. Phys. **A 668** (2000) 113.
3. E. Oset and L. L. Salcedo, Nucl. Phys. **A 443** (1985) 704.
4. Y. Sato, these proceedings.
5. U. Straub, J. Nieves, A. Faessler and E. Oset, Nucl. Phys. **A 556** (1993) 531.
6. T. Motoba and K. Itonaga, Prog. Theor. Phys. Suppl. **117** (1994) 477.
7. J. J. Szymanski *et al.*, Phys. Rev. **C 43** (1991) 849.
8. T. A. Armstrong *et al.*, Phys. Rev. **C 47** (1993) 1957.
9. H. Noumi *et al.*, Phys. Rev. **C 52** (1995) 2936.
10. P. Kulessa *et al.*, Phys. Lett. **B 427** (1998) 403; H. Ohm *et al.*, Phys. Rev. **C 55** (1997) 3062.
11. H. Park *et al.*, Phys. Rev. **C 61** (2000) 054004.